IEEE Access
Multidisciplinary ⋮ Rapid Review ⋮ Open Access Journal

Received 30 June 2024, accepted 13 July 2024, date of publication 16 July 2024, date of current version 24 July 2024.

Digital Object Identifier 10.1109/ACCESS.2024.3429405

RESEARCH ARTICLE

Optimal Scheduling Strategy for Energy Allocation of Distributed Electric Heat Storage

HUICHAO JI[1] **AND LEI WANG**[2]
[1]School of Automation Engineering, Northeast Electric Power University, Jilin 132012, China
[2]College of Information and Control Engineering, Jilin Institute of Chemical Technology, Jilin 132022, China

Corresponding author: Lei Wang (wanglei@jlict.edu.cn)

This work was supported by the Ph.D. Scientific Research Startup Foundation of Northeast Electric Power University under Grant BSJXM-2022209.

ABSTRACT Electric heat storage (EHS) located on the grid side can improve the flexibility of combined heat and power (CHP) systems to reduce wind power curtailment (WPC), and its capacity is correlated with investment costs. However, a significant amount of distributed electric heat storage (DEHS) on the load side has already been funded and constructed by users and businesses. To effectively utilize DEHS for diverse user types in different geographic locations, a generalized scheduling method is required to address these issues. To fill the technology gap, an innovative optimal scheduling strategy for energy allocation in DEHS is proposed. Firstly, to consider the heat comfort of DEHS users and their willingness to serve grid scheduling, the equivalent energy allocation strategy (EEAS) and increased energy allocation strategy (IEAS) are developed, respectively. Secondly, a general model is proposed to schedule DEHS for different types of users. The electric heat time-shift characteristics of DEHS are used to reallocate the working time of energy storage. Thirdly, numerical simulations are employed to validate the proposed strategy. The proposed scheduling strategies of EEAS and IEAS contribute to the reduction of WPC. The WPC rates are reduced by 14.04% and 29.49%, respectively, when compared to the conventional scheduling strategy of time-of-use. Moreover, compared with EEAS, IEAS makes a significant contribution by providing 27.05% more scheduling space for the grid, thus greatly improving its flexibility in consuming wind power. The WPC can be reduced through the energy allocation of DEHS, while the flexibility of grid regulation is enhanced by increasing the deviation of energy allocation.

INDEX TERMS Optimal scheduling, distributed electric heat storage, equivalent energy allocation strategy, increased energy allocation strategy.

NOMENCLATURE

ABBREVIATIONS

BES	Battery Energy Storage.
CHP	Combined Heat and Power.
DEHS	Distributed Electric Heat Storage.
EHS	Electric Heat Storage.
EEAS	Equivalent Energy Allocation Strategy.
HES	Heat Energy Storage.
HPP	Heat Power Plants.
IEAS	Increased Energy Allocation Strategy.
WPC	Wind Power Curtailment.
WPP	Wind Power Plants.

The associate editor coordinating the review of this manuscript and approving it for publication was Ayaz Ahmad.

I. INTRODUCTION

A. MOTIVATION

With massive wind power generation connected to the power grid, wind power accommodation has been a challenge for optimal power system scheduling [1], [2]. Due to the coupling characteristics between the electric and heat power output from combined heat and power (CHP) systems, the wind power accommodation is restricted [3]. It is urgent to adopt a

method to tackle the problem of wind power accommodation in the optimal scheduling of CHP. Since electric energy can be converted into heat energy by electric heat storage (EHS) during the load valley and released during the peak [4], [5], [6]. The electric heat time-shift characteristics are widely used to improve the flexibility of CHP and wind power accommodation [7]. However, the current distributed EHS, which is widely distributed in different geographical locations, is not effectively utilized by the grid to consume wind power. This is due to the diversity of user types involved. The technology gap has not been filled in the existing studies. Therefore, a method needs to be developed to schedule the distributed electric heat storage (DEHS).

B. LITERATURE REVIEW

Various control strategies of EHS are implemented to provide demand response service. EHS is typically integrated with CHP to improve renewable energy penetration [8], [9]. Eggers et al. [10] establish an EHS demonstration plant in Hamburg, Germany, and developed the idea of long-duration energy storage. The EHS is used to profoundly alleviate the instability of wind and solar energy. Ji et al. [11] present a hybrid heating system using off-peak EHS, which is conducive to realizing the graded utilization of energy and improving the system's energy efficiency. OhS et al. [12] explore a configuration of the EHS dedicated S-CO_2 recompression cycle that can improve the flexibility of conventional power plants, renewable energy curtailment, and securing ancillary services. Wang et al. [7] combine EHS and heat pumps in a CHP plant, and a regulation strategy is proposed to minimize the wind power curtailment (WPC) in a region with EHS and heat pumps. The WPC ratio is reduced from 20.31% to 13.04% and 7.51%, respectively. The results of the above studies prove that the EHS contributes to wind power accommodation. Furthermore, the EHS in the existing studies is primarily located on the grid side, and the EHS is directly scheduled by power plants or the grid without developing a specific scheduling strategy. However, the investment costs associated with the capacity of grid-side EHS increase the operating costs of the system. Additionally, this part of the EHS does not require further funding since it is built and invested in by individuals and businesses, and it operates on the load side for a long time. The above issues can be resolved through the effective utilization of DEHS.

To study DEHS on the load side, Buttitta et al. [4] investigate the effect of different control strategies applied to EHS to provide demand response services. The strategies are rule-based control, unconstrained model predictive control, and constrained model predictive control, respectively. Three case results point to the need for policymakers and manufacturers to focus on implementing advanced control for EHS systems. These controls should be applied to households with varying occupancy patterns, thereby making demand response initiatives more attractive to end users. These advanced controls should also be considered for auxiliary thermal network regulation (ATNR). Srithapon and Månsson [13] propose a two-stage energy management strategy that schedules electric vehicles in cooperation with heat pumps and EHS to enhance the flexibility of energy communities located on the load side. Rostamnezhad et al. [14] explain the total building electric power load consisting of fixed and shiftable loads, which can be transferred from peak hours to another time. For instance, electric boilers, chillers, and pumps can be considered as shiftable loads. Therefore, a unanimous consensus is obtained in existing studies that load-side resources are effective in improving system flexibility. However, a substantial number of DEHS on the load side for different types of users are not utilized [15], [16]. Therefore, this research presents a DEHS-based energy allocation strategy. Working with DEHS users, a scheduling protocol is developed that allows for these variances by assigning DEHS operating time according to variations in wind power output. Furthermore, the different heat comfort needs of different DEHS consumers are considered, leading to the creation of two optimal scheduling strategies: the equivalent energy allocation strategy (EEAS) and the increased energy allocation strategy (IEAS).

The above energy allocation strategy needs to be combined with the scheduling protocol signed by the user to reallocate the working time of energy storage for its DEHS. Therefore, it is necessary to establish an optimal scheduling model for energy allocation. Gomes and Vale [17] propose a costless renewable energy allocation model that considers each member's individual participation in demand response. The energy allocation model can distribute renewable energy in a fair and costless manner. This reference solves the allocation of community renewable energy among community members' buildings. Zare et al. [18] present a stochastic model to solve the collaborative expansion planning of modern multi-energy allocation networks. The electric vehicle charging stations are considered to optimize the charging time. Talat et al. [19] develop a novel blockchain-based decentralized green energy allocation system for trustless reliable energy exchanges in a smart grid. The energy allocation transfers energy by way of intermediaries, including smart generation devices, intelligent controllers, central grid, and others, in a decentralized manner. Ahn et al. [20] propose distributed energy generation and energy allocation laws. The law of energy allocation dictates that the charging and discharging of batteries be applied in a distributed process. These studies are entirely different from DEHS, the scheduling of different types of users' DEHS, the greater the deviation between the scheduling results and user expectations, the greater the flexibility of regulating the DEHS. However, to increase user willingness to participate in grid regulation and simultaneously consider heat comfort, unique models of energy allocation strategy are needed to solve this problem.

C. CONTRIBUTIONS AND PAPER ORGANIZATIONS

Due to the lack of an effective scheduling strategy, a substantial number of DEHS with electric heat time-shift

TABLE 1. Comparison between the proposed method and other methods*.

Comparison		Other methods												Proposed method
References		[7]	[10]	[11]	[12]	[13]	[14]	[15]	[16]	[17]	[18]	[19]	[20]	
Target	DEHS	✗	✗	✗	✗	✓	✓	✓	✓	✗	✗	✗	✗	✓
	EHS	✓	✓	✓	✓	✗	✗	✗	✗	✗	✗	✗	✗	✗
Location	Load side	✗	✗	✗	✗	✓	✓	✓	✓	✓	✓	✓	✓	✓
	Grid side	✓	✓	✓	✓	✗	✗	✗	✗	✗	✗	✗	✗	✗
Objectives	Reduce WPC	✓	✓	✗	✗	✗	✗	✓	✓	✗	✓	✓	✗	✓
	Minimum operation costs	✓	✗	✓	✓	✓	✓	✓	✓	✓	✓	✓	✓	✓
Constraints	User heat comfort	✗	✗	✗	✗	✓	✗	✓	✗	✗	✗	✗	✗	✓
	Different types of users	✗	✗	✗	✗	✓	✓	✓	✓	✓	✗	✓	✗	✓
Scheduling model	Energy allocation strategy	✗	✗	✗	✗	✗	✗	✗	✗	✓	✓	✓	✓	✓
	EEAS	✗	✗	✗	✗	✗	✗	✗	✗	✗	✗	✗	✗	✓
	IEAS	✗	✗	✗	✗	✗	✗	✗	✗	✗	✗	✗	✗	✓

*✓:The item is considered. ✗:The item is not considered.

characteristics located on the load side are not utilized. To fill the technology gap, this paper proposes an energy allocation strategy of DEHS, the comparison between the proposed method and other methods is shown in Table 1. The main contributions of this paper are given as follows:

- To the best of our knowledge, this is the first time that an energy allocation strategy of DEHS is proposed. The load-side DEHS is utilized to improve wind power accommodation and ensure user comfort;
- The models of EEAS and IEAS are established based on scheduling protocols signed by users, which can develop differentiated scheduling strategies based on the heat demand of different types of users and improve the willingness of users to participate in grid regulation;
- Compared with the conventional scheduling strategy of time-of-use, the WPC rates of EEAS and IEAS are reduced by 14.04% and 29.49%, respectively. The scheduling results of the two strategies are quantified using equation (41) to determine the contribution to grid regulation. The evaluation index ϑ for EEAS and IEAS is 2.07% and 2.63%, respectively. Compared with EEAS, IEAS can provide 27.05% more scheduling space for the grid to consume wind power.

The rest of this paper is organized as follows: The combined electricity and heat systems with DEHS are described in Section II. The energy allocation strategy of DEHS is proposed in Section III. The modeling of conventional power generation and electric and heat energy storage is presented in Section IV. The numerical simulations of three cases are validated in Section V. Section VI is the conclusion.

II. SYSTEM MODELING WITH DEHS

The system structure of the combined electricity and heat systems with DEHS is illustrated in Figure 1. The system consists of two layers, the upper and the lower layers, which are coordinated by a centralized communication network. The scheduling centre is responsible for implementing scheduling and control, as well as collecting and analyzing electrical load data within the upper layer. The electrical load data from DEHS is uploaded to the database via switches, and historical data stored in the database is employed to predict the power output of DEHS. The operational constraints of DEHS are provided to the scheduling centre to establish an energy allocation model. Finally, the optimized scheduling results are sent from the scheduling centre to DEHS through switches.

The lower layer of this system comprises several components, including wind power plants (WPP), heat power plants (HPP), battery energy storage (BES) units, CHP plants, heat energy storage (HES) systems such as hot water tanks, electric load, heat load, and a diverse range of DEHS catering to different types of users such as highway rest stops, suburban houses, manufactories, and shopping malls. Heat load is supplied by CHP and HES, with DEHS serving as auxiliary regulation in urban heat networks. HES functions to store excess heat energy generated by CHP, releasing it during periods of increased heat load demand. Electric load is powered by WPP, HPP, BES, and CHP, with BES storing electricity during low load periods and releasing it during peak demand. This electric energy is consumed by DEHS to generate heat energy, which is subsequently stored within DEHS. DEHS are categorized based on their allocation in suburban and urban areas. In suburban regions, highway rest stops, suburban houses, and manufactories are situated far from the district heating network, relying solely on DEHS to meet their heat demand. Conversely, in urban areas, the high heat demand of shopping malls is met through a combination of DEHS and district heating network.

As centralized electric heat storage units are often funded and constructed by entities such as power grids, power plants, or heating supply companies, the capacity of these units is inherently linked to investment costs. Therefore, the coordination of DEHS via a centralized communication network can significantly enhance the electric heat storage capacity, facilitate the integration of wind power, and decrease electricity costs for DEHS users, thereby fostering a mutually beneficial outcome.

III. ENERGY ALLOCATION STRATEGY OF DEHS

A. ASSUMPTION CONDITIONS OF ENERGY ALLOCATION STRATEGY

The implementation of the energy allocation strategy ought to take into account the willingness of DEHS users to

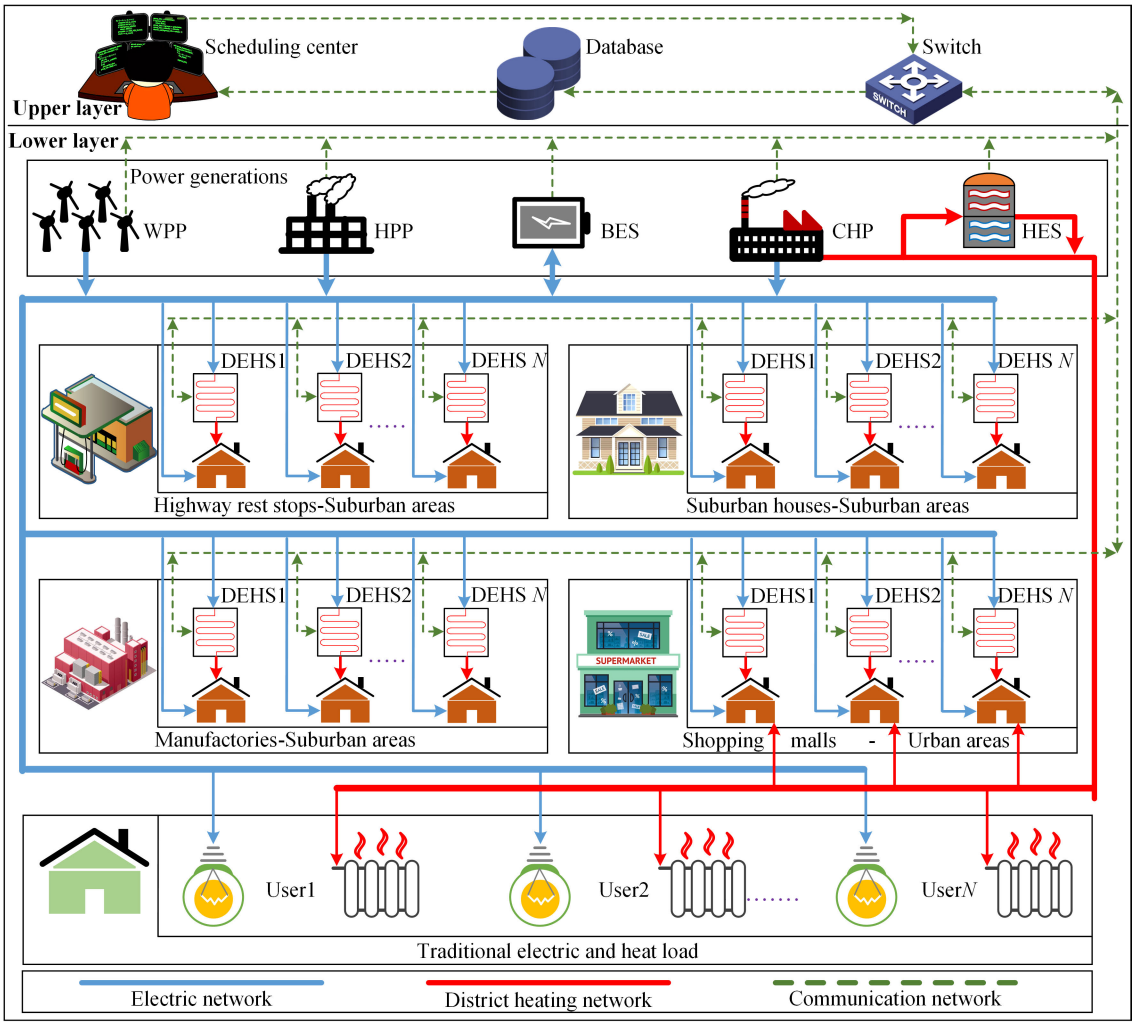

FIGURE 1. The structure of combined electricity and heat systems with DEHS.

engage in grid regulation. Ensuring grid scheduling flexibility while satisfying user heat storage demands necessitates the establishment of a deviation within the scheduling protocol. This deviation, pertaining to DEHS, represents the difference $\Delta\delta_{x,n}$ between the downward $\delta_{x,n,\text{down}}$ and upward $\delta_{x,n,\text{up}}$ limits of the average error between scheduled and predicted power. The magnitude of this deviation is inversely proportional to the depth of grid regulation for DEHS, with larger deviations resulting in higher scheduling subsidies for users. It is assumed that participating users have already entered into a scheduling protocol with the grid, and based on their specific conditions, have chosen a deviation within the protocol. Their DEHS operate as load-side resources, responding to grid regulation. Given the regular patterns in electricity consumption among DEHS users involved in energy allocation scheduling, the historical load curve of DEHS exhibits a different pattern of sudden increases and decreases. It is assumed that DEHS participating in the scheduling operates on an hourly basis, with only two operational states: start and stop.

An example is presented for the better understanding of the reader. In a smart community, the DEHS system serves approximately 1,000 residential users. Among these residents, there are different groups such as the elderly, housewives, office workers, and students, who have varying demands and timeframes for heating. Additionally, there is a small commercial centre and a school within the community, which have higher requirements for the stability and continuity of heating. Each resident's home is equipped with a DEHS device with a capacity of 10kWh. These devices utilize advanced phase change materials as the heat storage medium, enabling them to charge and store thermal energy during the low-price nighttime period and release it during peak daytime hours for household use. The specific operation mode is as follows:

- During the low-price period of electricity at night, the control system will activate the DEHS heat storage mode. At this time, the DEHS in residents' homes begins to absorb electric energy from the power grid and convert it into heat energy for storage;

- During the peak price period of electricity in the daytime, the control system will activate the heat release mode of DEHS. At this time, DEHS begins to release the stored heat energy to provide heating services for residents' homes, commercial centres, and schools. Meanwhile, based on users' heating needs and the power grid load conditions, the control system will adjust the heat release rate and temperature of the DEHS to ensure the comfort and stability of heating;
- When the power grid load is too high or the production of renewable energy is excessive, the central control system will activate the demand response mechanism. At this time, some DEHS will suspend charging or reduce the heat release rate to reduce the power grid load or consume excess renewable energy. Through this way, the DEHS can participate in the scheduling and balance of the power grid, improving the stability of the power grid.

B. THE DESCRIPTION OF ENERGY ALLOCATION STRATEGY

The schematic diagram of the energy allocation strategy for DEHS is presented in Figure 2. An example is selected to illustrate the operation of DEHS, and the changes in optimized scheduling based on time-of-use, EEAS, and IEAS are explained. Figure 2 (a) displays a schematic diagram based on time-of-use. According to the predicted power curve, the DEHS is scheduled during 0:00-7:00, 14:00-15:00, and 21:00-24:00. However, with time-of-use as the scheduling strategy, the DEHS is not scheduled during the 14:00-15:00 period. Due to peak and valley price constraints, when volatile scenarios of WPC arise, the regulatory flexibility of DEHS is restricted.

Figure 2 (b) is a schematic diagram of the EEAS. According to the predicted power curve, the DEHS stops operating from 7:00 to 8:00 and runs from 14:00 to 15:00, respectively. Suppose the wind power output is still large during the 7:00-8:00 period, further accommodation of wind power is required. However, the time-of-use strategy is not feasible, and thus, an energy allocation strategy needs to be employed. This strategy can reallocate the task of storing heat energy from 14:00 to 15:00 to the 7:00-8:00 period. Therefore, in contrast to time-of-use scheduling, EEAS regulates the operational time of the DEHS without altering the user's heat energy storage requirements, thereby enhancing the flexibility of wind power accommodation.

Figure 2 (c) is a schematic diagram of the IEAS. According to the predicted power curve, the DEHS stops operating during the periods of 2:00 to 3:00, 4:00 to 5:00, and 7:00 to 8:00. However, due to the increased deviations in the scheduling protocol signed by DEHS users, not only is the task of storing heat energy from 14:00 to 15:00 reallocated to 7:00 to 8:00, but also DEHS runs storing heat energy from 2:00 to 3:00 and 4:00 to 5:00. Therefore, compared to the EEAS, the increased operating hours of DEHS, within the range of scheduling deviations tolerable by users, allows the system to improve the flexibility of wind power accommodation.

C. THE FRAMEWORK OF ENERGY ALLOCATION STRATEGY

The framework of the energy allocation strategy is depicted in Figure 3, where the inputs consist of electric and heat load data along with predicted wind power. Within this model, the determination of whether the deviation $\Delta\delta_{x,n}$ equals zero dictates the allocation approach. Specifically, when

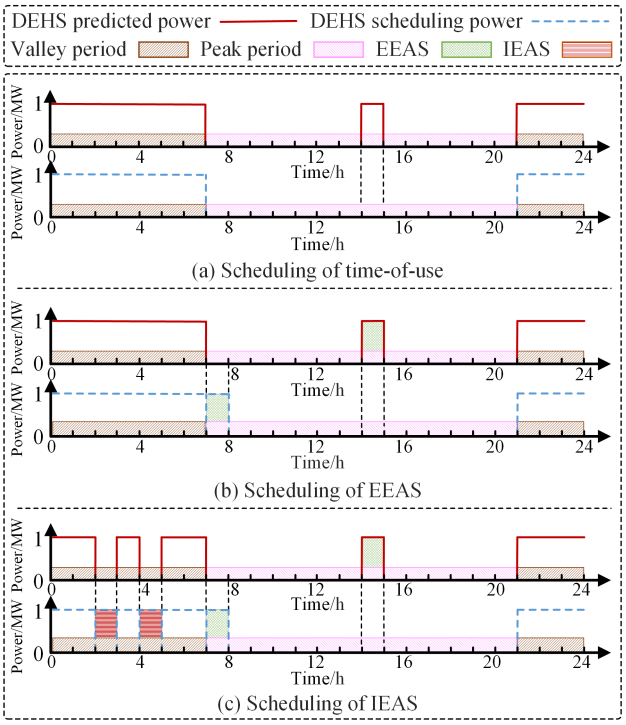

FIGURE 2. The schematic diagram of energy allocation strategy in DEHS.

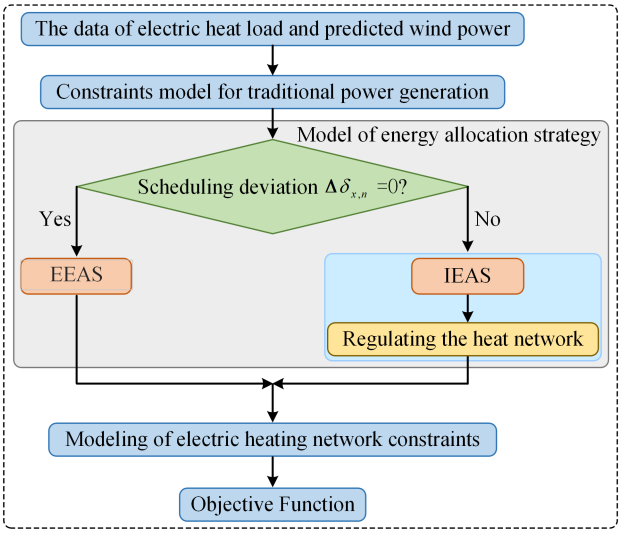

FIGURE 3. The model framework of energy allocation strategy.

$\Delta\delta_{x,n}$ is zero, EEAS is employed for DEHS. Conversely, if $\Delta\delta_{x,n}$ exceeds zero, IEAS is implemented, with the excess heat energy stored serving as a means to regulate the heat network. By integrating conventional power generation unit models with electric heat network constraint models, optimal scheduling is achieved, aiming to mitigate WPC and minimize operational costs within the system.

D. THE ENERGY ALLOCATION MODEL OF DEHS

1) OPERATION COST OF DEHS

The operating costs of DEHS require consideration of both scheduling and user electricity costs, as presented in (1)-(5). These include:

- The operating costs pertaining to peak and valley electricity prices are designated as $C^{\mathrm{a}}_{x,n,t}$, with the real cost of electricity during peak and valley periods being used to calculate DEHS scheduling costs;
- The operating cost associated with peak and valley subsidies are represented by $C^{\mathrm{b}}_{x,n,t}$. These subsidies are awarded for the scheduling power of DEHS that exceeds the user's actual demand, taking into account the specific peak and valley periods;
- The operating cost designated as $C^{\mathrm{c}}_{x,n,t}$ corresponds to the penalty imposed for scheduling deficits. When the scheduling result falls below the user's actual demand, leading to a reduction in heat comfort, a corresponding penalty is levied;
- The operating cost related to the incentive for regulating the heat network is denoted by $C^{\mathrm{d}}_{x,n,t}$. Since the excess energy stored in the IEAS of DEHS is utilized for heat network regulation, the power generated by the IEAS is already subsidized. Therefore, a consistent incentive is implemented to reward users during the scheduling periods.

$$C^{\mathrm{DEHS}}\left(P_{x,n,t}, H_{x,n,t}\right) = C^{\mathrm{a}}_{x,n,t} + C^{\mathrm{b}}_{x,n,t} + C^{\mathrm{c}}_{x,n,t} + C^{\mathrm{d}}_{x,n,t} \quad \forall x \in \mathcal{I}^{\mathrm{DEHS}}, n \in N_x, t \in \mathcal{T} \tag{1}$$

where $C^{\mathrm{DEHS}}(\cdot)$ is the cost function of DEHS, $P_{x,n,t}$ and $H_{x,n,t}$ are the scheduled electric and heat power of the nth DEHS of type x at time t. $C^{\mathrm{a}}_{x,n,t}$, $C^{\mathrm{b}}_{x,n,t}$, $C^{\mathrm{c}}_{x,n,t}$ and $C^{\mathrm{d}}_{x,n,t}$ denote the operating costs of the nth DEHS of type x at time t for four parts: peak and valley electricity prices, peak and valley electricity subsidies, scheduling shortage penalty and regulation heat network reward, respectively. Set $\mathcal{I}^{\mathrm{DEHS}}$ represents the indices for the user types of DEHS, set $\mathcal{N}_x$ represents the indices for users of type x in DEHS, and set $\mathcal{T}$ represents the indices of scheduling periods.

$$C^{\mathrm{a}}_{x,n,t} = \xi^{\mathrm{a}}_t P_{x,n,t} \quad \forall x \in \mathcal{I}^{\mathrm{DEHS}}, n \in N_x, t \in \mathcal{T} \tag{2}$$

$$C^{\mathrm{b}}_{x,n,t} = \xi^{\mathrm{b}}_t \left|P_{x,n,t} - P^{\mathrm{p}}_{x,n,t}\right| \varepsilon^{\mathrm{q}}_{x,n,t} \quad \forall x \in \mathcal{I}^{\mathrm{DEHS}}, n \in N_x, t \in \mathcal{T} \tag{3}$$

$$C^{\mathrm{c}}_{x,n,t} = \xi^{\mathrm{c}}_t \left|P_{x,n,t} - P^{\mathrm{p}}_{x,n,t}\right| \left(1 - \varepsilon^{\mathrm{q}}_{x,n,t}\right) \quad \forall x \in \mathcal{I}^{\mathrm{DEHS}}, n \in N_x, t \in \mathcal{T} \tag{4}$$

$$C^{\mathrm{d}}_{x,n,t} = \xi^{\mathrm{d}}_t \frac{\sum_{t\in\mathcal{T}} H^{\mathrm{p}}_{x,n,t} - \sum_{t\in\mathcal{T}} H_{x,n,t}}{\beta_{x,n}} \quad \forall x \in \mathcal{I}^{\mathrm{DEHS}}, n \in N_x, t \in \mathcal{T} \tag{5}$$

where ξ^{a}_t, ξ^{b}_t, ξ^{c}_t and ξ^{d}_t are the electricity prices of the four parts at time t, respectively. $\varepsilon^{\mathrm{q}}_{x,n,t}$ is the binary variable associated with scheduling shortage of the nth DEHS of type x at time t. $P^{\mathrm{p}}_{x,n,t}$ and $H^{\mathrm{p}}_{x,n,t}$ are the predicted electric power and heat power of the nth DEHS of type x at time t. $\beta_{x,n}$ is the electric heat conversion efficiency of the nth DEHS of type x. $\varepsilon^{\mathrm{q}}_{x,n,t} = 1$ if$\left(\sum_{t\in\mathcal{T}} P_{x,n,t} \geq \sum_{t\in\mathcal{T}} P^{\mathrm{p}}_{x,n,t}\right)$, $\varepsilon^{\mathrm{q}}_{x,n,t} = 0$ if$\left(\sum_{t\in\mathcal{T}} P_{x,n,t} < \sum_{t\in\mathcal{T}} P^{\mathrm{p}}_{x,n,t}\right)$.

2) ENERGY ALLOCATION CONSTRAINTS OF ELECTRIC POWER

The scheduling deviation constraints pertaining to both EEAS and IEAS within DEHS are presented in (6).

$$\delta_{x,n,\mathrm{down}} \leq \frac{\sum_{t\in\mathcal{T}} \left|P_{x,n,t}\varepsilon_{x,n,t} - P^{\mathrm{p}}_{x,n,t}\right|}{24} \leq \delta_{x,n,\mathrm{up}} \quad \forall x \in \mathcal{I}^{\mathrm{DEHS}}, n \in N_x \tag{6}$$

where $\delta_{x,n,\mathrm{down}}$ and $\delta_{x,n,\mathrm{up}}$ are the downward and upward limits of the deviation of the nth DEHS of type x. $\varepsilon_{x,n,t}$ is the binary variable associated with start-stop of the nth DEHS of type x at time t, $\varepsilon_{x,n,t} \in \{0, 1\}$, start is 1, stop is 0.

To reflect the discrepancy between the scheduled power and the demand power of DEHS users, the scheduling result deviation coefficient is devised, serving as a guiding metric for district heating network regulation. Its calculation is detailed in (7).

$$\frac{\sum_{t\in\mathcal{T}} P_{x,n,t}}{\sum_{t\in\mathcal{T}} P^{\mathrm{p}}_{x,n,t}} = \alpha_{x,n} \quad \forall x \in \mathcal{I}^{\mathrm{DEHS}}, n \in N_x \tag{7}$$

where $\alpha_{x,n}$ is the ratio of the total amount of scheduling and demand for the nth DEHS of type x, $\alpha_{x,n} > 1$ indicates that the total scheduling exceeds the demand, whereas $\alpha_{x,n} \leq 1$ signifies that the scheduling is less than or equal to the demand. Additionally, $\sum_{t\in\mathcal{T}} P^{\mathrm{p}}_{x,n,t}$ represents the aggregate of the predicted power for DEHS, a fixed value determined through day-ahead prediction.

The scheduling power constraint of DEHS is expressed as (8).

$$P_{x,n,\min} \leq P_{x,n,t}\varepsilon_{x,n,t} \leq P_{x,n,\max} \quad \forall x \in \mathcal{I}^{\mathrm{DEHS}}, n \in N_x, t \in \mathcal{T} \tag{8}$$

where $P_{x,n,\min}$ and $P_{x,n,\max}$ are the minimum and maximum electric power limits of the nth DEHS of type x.

3) ENERGY ALLOCATION CONSTRAINTS OF HEAT POWER

The IEAS of DEHS for regulating the heat network is constrained by (9) and (10).

$$H^{\mathrm{p}}_{x,n,t} = \beta_{x,n} P^{\mathrm{p}}_{x,n,t} \quad \forall x \in \mathcal{I}^{\mathrm{DEHS}}, n \in N_x, t \in \mathcal{T} \tag{9}$$

$$0 \leq H_{x,n,t} \leq H^{\mathrm{p}}_{x,n,t} \quad \forall x \in \mathcal{I}^{\mathrm{DEHS}}, n \in N_x, t \in \mathcal{T} \tag{10}$$

When the deviation coefficient $\alpha_{x,n}$ exceeds 1, the excess heat energy stored in DEHS is utilized, and the scheduling heat power is subject to the constraint presented in (11).

$$\frac{\sum_{t\in\mathcal{T}} H^{\mathrm{p}}_{x,n,t} - \sum_{t\in\mathcal{T}} H_{x,n,t}}{\beta_{x,n}} \le \left(\alpha_{x,n}-1\right)\sum_{t\in\mathcal{T}} P^{\mathrm{p}}_{x,n,t} \quad \forall x \in \mathcal{I}^{\mathrm{DEHS}}, n \in N_x \tag{11}$$

IV. MODELING OF TRADITIONAL POWER GENERATION, ELECTRIC AND HEAT ENERGY STORAGE

A. MODELING OF HPP

1) OPERATION COST OF HPP

The fuel cost of HPP, which is employed for regulating electric power, is expressed in (12).

$$C^{\mathrm{HPP}}\left(P_{f,t}\right) = \xi_{f,0}\left(P_{f,t}\right)^2 + \xi_{f,1}P_{f,t} + \xi_{f,2} \quad \forall f \in \mathcal{I}^{\mathrm{HPP}}, t \in \mathcal{T} \tag{12}$$

where $C^{\mathrm{HPP}}(\cdot)$ is the cost function of HPP. $P_{f,t}$ is the scheduled electric power of the fth HPP at time t. $\xi_{f,0}$, $\xi_{f,1}$ and $\xi_{f,2}$ are the operating cost coefficients of the fth HPP, respectively. Set $\mathcal{I}^{\mathrm{HPP}}$ represents the indices of HPP.

2) CONSTRAINTS OF HPP

The minimum and maximum power output limits, as well as the ramp rate constraints of the HPP, are detailed in (13) and (14).

$$P_{f,\min} \le P_{f,t} \le P_{f,\max} \quad \forall f \in \mathcal{I}^{\mathrm{HPP}}, t \in \mathcal{T} \tag{13}$$

$$R_{f,\mathrm{down}} \times \Delta t \le P_{f,t} - P_{f,t-1} \le R_{f,\mathrm{up}} \times \Delta t \quad \forall f \in \mathcal{I}^{\mathrm{HPP}}, t \in \mathcal{T} \tag{14}$$

where $P_{f,\min}$ and $P_{f,\max}$ are the minimum and maximum electric power limits of the fth HPP. $R_{f,\mathrm{down}}$ and $R_{f,\mathrm{up}}$ are the downward and upward ramp rate limits of the fth HPP. Δt is the scheduling interval.

B. MODELING OF CHP AND HES

1) OPERATION COSTS OF CHP AND HES

The fuel cost of CHP, along with the operational and investment costs pertaining to the charge and discharge processes of HES, are presented in (15) and (16).

$$C^{\mathrm{CHP}}\left(P_{b,t}, H_{b,t}\right) = \xi_{b,0}\left[P_{b,t} + v_b H_{b,t}\right]^2 + \xi_{b,1}\left[P_{b,t} + v_b H_{b,t}\right] + \xi_{b,2} \quad \forall b \in \mathcal{I}^{\mathrm{CHP}}, t \in \mathcal{T} \tag{15}$$

$$C^{\mathrm{HES}}\left(H^+_{k,t}, H^-_{k,t}\right) = \xi_{k,0}\left(H^+_{k,t} + H^-_{k,t}\right) + \left[\left(\xi_{k,1}H_{k,\mathrm{rated}} + \xi_{k,2}S_{k,\max}\right)/T_k\right] \quad \forall k \in \mathcal{I}^{\mathrm{HES}}, t \in \mathcal{T} \tag{16}$$

where $C^{\mathrm{CHP}}(\cdot)$ is the cost function of CHP. $P_{b,t}$ and $H_{b,t}$ are the scheduled electric and heat power of the bth CHP at time t, respectively. $\xi_{b,0}$, $\xi_{b,1}$ and $\xi_{b,2}$ are the operating cost coefficients of the bth CHP, respectively. v_b is the reduction in power generation when the bth CHP extracts per unit of heat with a constant air intake. Set $\mathcal{I}^{\mathrm{CHP}}$ represents the indices of CHP. $C^{\mathrm{HES}}(\cdot)$ is the cost function of HES. $H^+_{k,t}$ and $H^-_{k,t}$ are the charge and discharge heat power of the kth HES at time t, respectively. $\xi_{k,0}$, $\xi_{k,1}$ and $\xi_{k,2}$ are the operation and maintenance, rated power and capacity cost coefficients of the kth HES. $H_{k,\mathrm{rated}}$, $S_{k,\max}$ and T_k are the rated power, maximum storage capacity and service life of the kth HES. Set $\mathcal{I}^{\mathrm{HES}}$ represents the indices of HES.

2) CONSTRAINTS OF CHP

The electric and heat power constraints, as well as the ramp rate limitations of CHP, are presented in (17)-(20).

$$\left(P_{b,\min} - v_{b,0}H_{b,t}\right) \le P_{b,t} \le \left(P_{b,\max} - v_{b,2}H_{b,t}\right) \quad \forall b \in \mathcal{I}^{\mathrm{CHP}}, t \in \mathcal{T} \tag{17}$$

$$v_{b,1}\left(H_{b,t} - H_{b,\mathrm{med}}\right) \le P_{b,t} \quad \forall b \in \mathcal{I}^{\mathrm{CHP}}, t \in \mathcal{T} \tag{18}$$

$$0 \le H_{b,t} \le H_{b,\max} \quad \forall b \in \mathcal{I}^{\mathrm{CHP}}, t \in \mathcal{T} \tag{19}$$

$$R_{b,\mathrm{down}} \times \Delta t \le P_{b,t} - P_{b,t-1} \le R_{b,\mathrm{up}} \times \Delta t \forall b \in \mathcal{I}^{\mathrm{CHP}}, t \in \mathcal{T} \tag{20}$$

where $P_{b,\min}$ and $P_{b,\max}$ are the minimum and maximum electric power limits of the bth CHP, $v_{b,0}$ and $v_{b,2}$ are the minimum and maximum reduction of the bth CHP, $v_{b,1}$ is the reduction of the bth CHP, $H_{b,\mathrm{med}}$ and $H_{b,\max}$ are the corresponding heat power when the bth CHP generates the minimum electric power and the maximum heat power limit of the bth CHP, $R_{b,\mathrm{down}}$ and $R_{b,\mathrm{up}}$ are the downward and upward ramp rate limits of the bth CHP.

3) CONSTRAINTS OF HES

The specifics of HES's heat power and heat energy storage capacity restrictions are covered in (21)-(27).

$$S_{k,t} = \beta_k S_{k,t-1} + H^+_{k,t} - H^-_{k,t} \quad \forall k \in \mathcal{I}^{\mathrm{HES}}, t \in \mathcal{T} \tag{21}$$

$$0 \le S_{k,t} \le S_{k,\max} \quad \forall k \in \mathcal{I}^{\mathrm{HES}}, t \in \mathcal{T} \tag{22}$$

$$H^+_{k,t} + S_{k,t-1} \le S_{k,\max} \quad \forall k \in \mathcal{I}^{\mathrm{HES}}, t \in \mathcal{T} \tag{23}$$

$$H^-_{k,t} - S_{k,t-1} \le 0 \quad \forall k \in \mathcal{I}^{\mathrm{HES}}, t \in \mathcal{T} \tag{24}$$

$$0 \le H^+_{k,t} \le H_{k,\mathrm{rated}}\varepsilon^+_{k,t} \quad \forall k \in \mathcal{I}^{\mathrm{HES}}, t \in \mathcal{T} \tag{25}$$

$$0 \le H^-_{k,t} \le H_{k,\mathrm{rated}}\varepsilon^-_{k,t} \quad \forall k \in \mathcal{I}^{\mathrm{HES}}, t \in \mathcal{T} \tag{26}$$

$$\varepsilon^+_{k,t} + \varepsilon^-_{k,t} \le 1 \quad \forall \varepsilon^+_{k,t}, \varepsilon^-_{k,t} \in \{0,1\}, k \in \mathcal{I}^{\mathrm{HES}}, t \in \mathcal{T} \tag{27}$$

where $S_{k,t}$ is the heat energy storage capacity of the kth HES at time t, β_k is the heat energy storage efficiency of the kth HES, $\varepsilon^+_{k,t}$ and $\varepsilon^-_{k,t}$ are the binary variable associated with charge and discharge of the kth HES at time t, $\varepsilon^+_{k,t} + \varepsilon^-_{k,t} \le 1$ stipulates that the kth HES is incapable of performing both charging and discharging operations concurrently at time t.

C. MODELING OF WPP

1) OPERATION COST OF WPP

The operational cost of WPP serves as a penalty for WPC, as indicated in (28).

$$C^{\mathrm{WPP}}\left(P_{g,t}\right)=\xi_{g,0}\left(\bar{P}_{g,t}-P_{g,t}\right)\forall g\in\mathcal{I}^{\mathrm{WPP}},t\in\mathcal{T}\quad(28)$$

where $C^{\mathrm{WPP}}(\cdot)$ is the cost function of WPP, $P_{g,t}$ is the electric power of the gth WPP at time t, $\xi_{g,0}$ is the WPC penalty cost of the gth WPP at time t, $\bar{P}_{g,t}$ is the predicted wind power output of the gth WPP at time t. Set $\mathcal{I}^{\mathrm{WPP}}$ represents the indices of WPP.

2) CONSTRAINT OF WPP

The upper limit of WPP output power is shown in (29).

$$0\le P_{g,t}\le\bar{P}_{g,t}\quad\forall g\in\mathcal{I}^{\mathrm{WPP}},t\in\mathcal{T}\quad(29)$$

D. MODELING OF BES

1) OPERATION COST OF BES

The costs associated with the charge and discharge operations, as well as the investment costs of BES, are detailed in (30).

$$\begin{aligned}C^{\mathrm{BES}}\left(P^{+}_{q,t},P^{-}_{q,t}\right)&=\xi_{q,0}\left(P^{+}_{q,t}+P^{-}_{q,t}\right)\\&+\left[\left(\xi_{q,1}P_{q,\mathrm{rated}}+\xi_{q,2}S_{q,\max}\right)/T_q\right]\\&\forall q\in\mathcal{I}^{\mathrm{BES}},t\in\mathcal{T}\end{aligned}\quad(30)$$

where $C^{\mathrm{BES}}(\cdot)$ is the cost function of BES. $P^{+}_{q,t}$ and $P^{-}_{q,t}$ are the charge and discharge electric power of the qth BES at time t, respectively. $\xi_{q,0}$, $\xi_{q,1}$ and $\xi_{q,2}$ are the operation and maintenance, rated power and capacity cost coefficients of the qth BES. $P_{q,\mathrm{rated}}$, $S_{q,\max}$ and T_q are the rated power, maximum storage capacity and service life of the qth BES. Set $\mathcal{I}^{\mathrm{BES}}$ represents the indices of BES.

2) CONSTRAINTS OF BES

The constraints pertaining to the rated electric power and capacity of BES are presented in (31)-(37).

$$S_{q,t}=\beta_q S_{q,t-1}+P^{+}_{q,t}-P^{-}_{q,t}\quad\forall q\in\mathcal{I}^{\mathrm{BES}},t\in\mathcal{T}\quad(31)$$

$$0\le S_{q,t}\le S_{q,\max}\quad\forall q\in\mathcal{I}^{\mathrm{BES}},t\in\mathcal{T}\quad(32)$$

$$P^{+}_{q,t}+S_{q,t-1}\le S_{q,\max}\quad\forall q\in\mathcal{I}^{\mathrm{BES}},t\in\mathcal{T}\quad(33)$$

$$P^{-}_{q,t}-S_{q,t-1}\quad\forall q\in\mathcal{I}^{\mathrm{BES}},t\in\mathcal{T}\quad(34)$$

$$0\le P^{+}_{q,t}\le P_{q,\mathrm{rated}}\varepsilon^{+}_{q,t}\quad\forall q\in\mathcal{I}^{\mathrm{BES}},t\in\mathcal{T}\quad(35)$$

$$0\le P^{-}_{q,t}\le P_{q,\mathrm{rated}}\varepsilon^{-}_{q,t}\quad\forall q\in\mathcal{I}^{\mathrm{BES}},t\in\mathcal{T}\quad(36)$$

$$\varepsilon^{+}_{q,t}+\varepsilon^{-}_{q,t}\le 1\quad\forall\varepsilon^{+}_{q,t},\varepsilon^{-}_{q,t}\in\{0,1\},q\in\mathcal{I}^{\mathrm{BES}},t\in\mathcal{T}\quad(37)$$

where $S_{q,t}$ is the electric energy storage capacity of the qth BES at time t, β_q is the electric energy storage efficiency of the qth BES, $\varepsilon^{+}_{q,t}$ and $\varepsilon^{-}_{q,t}$ are the binary variable associated with charge and discharge of the qth BES at time t, $\varepsilon^{+}_{q,t}+\varepsilon^{-}_{q,t}\le 1$ stipulates that the qth BES is incapable of performing both charging and discharging operations concurrently at time t.

E. OPTIMIZATION OBJECTIVES, ELECTRIC-HEAT NETWORK CONSTRAINTS

1) OPTIMIZATION OBJECTIVE

The objective function for day-ahead optimal scheduling, aimed at mitigating WPC and minimizing system operational costs, is presented in (38).

$$\begin{aligned}\mathrm{Min}C=&\sum_{t\in\mathcal{T}}\sum_{x\in\mathcal{I}^{\mathrm{DEHS}}}\sum_{n\in N_x}C^{\mathrm{DEHS}}\left(P_{x,n,t},H_{x,n,t}\right)\\&+\sum_{t\in\mathcal{T}}\sum_{f\in\mathcal{I}^{\mathrm{HPP}}}C^{\mathrm{HPP}}\left(P_{f,t}\right)+\sum_{t\in\mathcal{T}}\sum_{g\in\mathcal{I}^{\mathrm{WPP}}}C^{\mathrm{WPP}}\left(P_{g,t}\right)\\&+\sum_{t\in\mathcal{T}}\sum_{b\in\mathcal{I}^{\mathrm{CHP}}}C^{\mathrm{CHP}}\left(P_{b,t},H_{b,t}\right)\\&+\sum_{t\in\mathcal{T}}\sum_{k\in\mathcal{I}^{\mathrm{HES}}}C^{\mathrm{HES}}\left(H^{+}_{k,t},H^{-}_{k,t}\right)\\&+\sum_{t\in\mathcal{T}}\sum_{q\in\mathcal{I}^{\mathrm{BES}}}C^{\mathrm{BES}}\left(P^{+}_{q,t},P^{-}_{q,t}\right)\end{aligned}\quad(38)$$

2) ELECTRIC NETWORK BALANCE CONSTRAINT

To uphold a harmonious equilibrium between the grid and the load within the electrical network, it is imperative to fulfil the constraint stated in (39).

$$\begin{aligned}&\sum_{f\in\mathcal{I}^{\mathrm{HPP}}}P_{f,t}+\sum_{b\in\mathcal{I}^{\mathrm{CHP}}}P_{b,t}+\sum_{g\in\mathcal{I}^{\mathrm{WPP}}}P_{g,t}-\sum_{q\in\mathcal{I}^{\mathrm{BES}}}P^{+}_{q,t}\\&+\sum_{q\in\mathcal{I}^{\mathrm{BES}}}P^{-}_{q,t}-\sum_{x\in\mathcal{I}^{\mathrm{DEHS}}}\sum_{n\in N_x}P_{x,n,t}=P^{\mathrm{L}}_{t}\quad\forall t\in\mathcal{T}\end{aligned}\quad(39)$$

where P^{L}_{t} is the electric load at time t.

3) HEAT NETWORK IMBALANCE CONSTRAINT

Due to the heat inertia of the circulating water in the heat network and structures, the heat load is maintained within a specified range to fulfil the heating demands of users. The restriction about the heat network imbalance is explained in (40).

$$\begin{aligned}\kappa_{\mathrm{low}}H^{\mathrm{L}}_{t}\le&\sum_{b\in\mathcal{I}^{\mathrm{CHP}}}H_{b,t}-\sum_{k\in\mathcal{I}^{\mathrm{HES}}}H^{+}_{k,t}+\sum_{k\in\mathcal{I}^{\mathrm{HES}}}H^{-}_{k,t}\\&+\sum_{x\in\mathcal{I}^{\mathrm{DEHS}}}\sum_{n\in N_x}H_{x,n,t}\le\kappa_{\mathrm{up}}H^{\mathrm{L}}_{t}\quad\forall t\in\mathcal{T}\end{aligned}\quad(40)$$

where κ_{low} and κ_{up} are the lower and upper limits of the thermal inertia regulation ratio of the district heating network and the building, and the κ_{low} and κ_{up} are 0.9 and 1.1, respectively. H^{L}_{t} is the heat load at time t.

F. QUANTIFICATION OF SCHEDULING RESULTS FOR DIFFERENT DEVIATION

To assess the influence of load-side resources on the depth of grid regulation, a quantitative analysis is conducted on the varying contributions of DEHS to grid regulation. References [21] and [22] analyze the regulation of peak loads and wind power accommodation capacity, providing insights into the grid's interaction with load-side resources. Building

on these findings, an evaluation index ϑ is introduced to measure load-side resource management. The evaluation index ϑ in this paper is only based on previous research work [21], [22], and no improvements have been made to this index. This index represents the sum of the scheduling power contributed by the four types of DEHS users, normalized by the total power accommodated by wind power. Therefore, the simulation case yields the contribution value of DEHS to grid regulation for wind power accommodation. The evaluation index ϑ is formally expressed in (41).

$$\vartheta = \sum_{t\in\mathcal{T}}\sum_{x\in\mathcal{I}^{\mathrm{DEHS}}}\sum_{n\in N_x} P_{x,n,t} \Big/ \sum_{t\in\mathcal{T}}\sum_{g\in\mathcal{I}^{\mathrm{WPP}}} P_{g,t}$$
$$\forall x \in \mathcal{I}^{\mathrm{DEHS}}, n \in N_x, g \in \mathcal{I}^{\mathrm{WPP}} \tag{41}$$

V. CASE STUDIES

The simulation data are obtained from the actual operational records of DEHS in a provincial power grid. The simulations are performed on a machine equipped with an Intel Core i5 CPU and 8 GB of memory. The modeling process is facilitated by MATLAB-R2018a and the YALMIP toolbox, with the IBM CPLEX optimizer used to solve the Mixed-Integer Quadratic Programming model.

A. THE SIMULATION STRUCTURE AND DATA

The structure diagram of the simulation structure of the combined electricity and heat systems with DEHS is represented in Figure 4. The simulation framework encompasses HPP_1 and HPP_2, CHP_1 and CHP_2, WPP, BES, HES_1 and HES_2, along with DEHS units tailored for four user: highway rest stops $\mathcal{I}_1^{\mathrm{DEHS}}$, suburban houses $\mathcal{I}_2^{\mathrm{DEHS}}$, manufactories $\mathcal{I}_3^{\mathrm{DEHS}}$, and shopping malls $\mathcal{I}_4^{\mathrm{DEHS}}$. For each user type $x \in \{1, 2, 3, 4\}$, i.e., $N_x = 4$, resulting in a total of 16 DEHS units. The detailed simulation data for HPPs, HESs, CHPs, BES, and DEHS, as referenced in the literature [15], [23], [24], [25], are shown in Table 2.

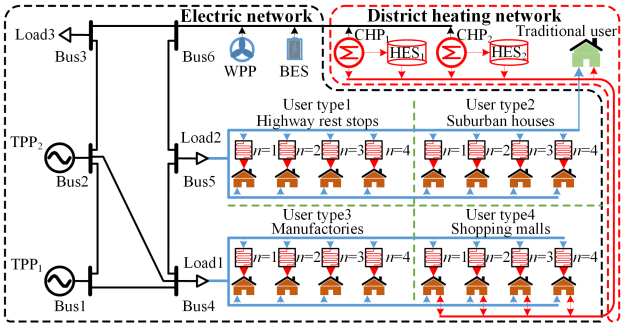

FIGURE 4. The structure diagram of the simulation structure of the combined electricity and heat systems with DEHS.

The curves for predicted wind power, electric and heat load are depicted in Figure 5. Given the positive correlation between human activities and electric load, as well as the inverse relationship between heat load and environmental

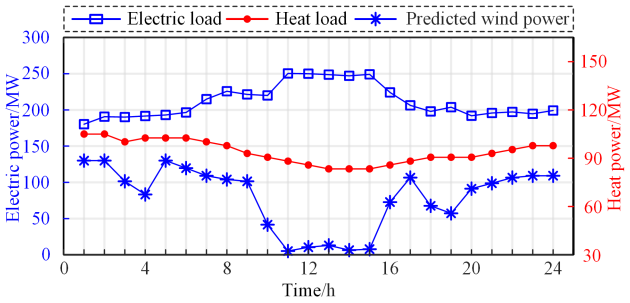

FIGURE 5. Curves of predicted wind power, electric and heat load.

temperature, it is observed that the peak of electric load occurs during periods opposite to that of heat load.

The predicted power curves for the four types of DEHS users are presented in Figure 6. To derive these curves, the prediction method combining the upper-lower approach with the iterative dichotomiser 3 algorithm from our prior research is employed. For a comprehensive understanding of the prediction method, the reader is advised to refer to [15].

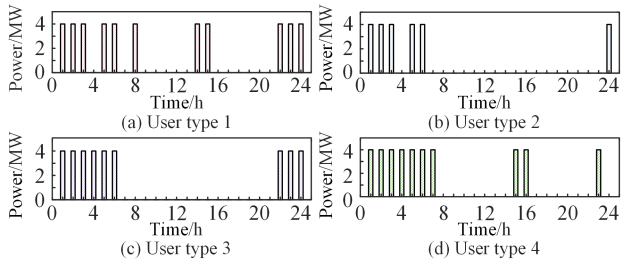

FIGURE 6. The predicted power of four types of DEHS users.

B. VALIDATION OF ENERGY ALLOCATION STRATEGY

To validate the effectiveness of the energy allocation strategy for DEHS, a comparative analysis of three cases is undertaken, as detailed subsequently.

- Case 1: Optimal scheduling of DEHS based on the conventional time-of-use prices strategy, the DEHS responds to grid demands to absorb wind power according to time-of-use prices. The operating cost of DEHS is calculated using peak and valley electricity prices $C^{\mathrm{a}}_{x,n,t}$, $C^{\mathrm{b}}_{x,n,t} = C^{\mathrm{c}}_{x,n,t} = C^{\mathrm{d}}_{x,n,t} = 0$.
- Case 2: Implementation of EEAS for DEHS, the DEHS is controlled based on the deviation of scheduling protocol $\delta_{x,n,\mathrm{down}} = \delta_{x,n,\mathrm{up}} = 0$. Since EEAS does not regulate the heat network, the operating cost of DEHS does not include the regulating the heat network incentive $C^{\mathrm{d}}_{x,n,t} = 0$.
- Case 3: Implementation of IEAS for DEHS. Improving the depth of regulation of DEHS based on Case 2. One-fifth of the DEHS heat storage capacity can be used as the regulation range when the DEHS user allows the $\Delta\delta_{x,n}$ to fluctuate within a certain range. The deviation of scheduling protocol is set to $\delta_{x,n,\mathrm{down}} = 0$, $\delta_{x,n,\mathrm{up}} = 0.2$.

TABLE 2. The simulation data.

Units	Symbol	Value	Symbol	Value	Symbol	Value	Symbol	Value
HPP_1	$P_{f,\min}$	10(MW)	$P_{f,\max}$	200(MW)	$R_{f,\text{down}}$	49.8(MW/h)	$R_{f,\text{up}}$	49.8(MW/h)
	$\xi_{f,0}$	0.00049($/MW^2)	$\xi_{f,1}$	16.833($/MW)	$\xi_{f,2}$	220.576($)		
HPP_2	$P_{f,\min}$	50(MW)	$P_{f,\max}$	200(MW)	$R_{f,\text{down}}$	40.2(MW/h)	$R_{f,\text{up}}$	40.2(MW/h)
	$\xi_{f,0}$	0.00125($/MW^2)	$\xi_{f,1}$	40.623($/MW)	$\xi_{f,2}$	161.868($)		
CHP_1	$P_{b,\min}$	10(MW)	$P_{b,\max}$	200(MW)	$R_{b,\text{down}}$	5(MW/h)	$R_{b,\text{up}}$	5(MW/h)
	$\xi_{b,0}$	0.00435($/MW^2)	$\xi_{b,1}$	3.6($/MW)	$\xi_{b,2}$	100($)	$H_{b,\text{med}}$	40(MW)
	$H_{b,\max}$	55(MW)	$v_{b,0}$	-0.25	$v_{b,1}$	2.33	$v_{b,2}$	-0.27
	v_b	0.15						
CHP_2	$P_{b,\min}$	10(MW)	$P_{b,\max}$	200(MW)	$R_{b,\text{down}}$	20(MW/h)	$R_{b,\text{up}}$	20(MW/h)
	$\xi_{b,0}$	0.00435($/MW^2)	$\xi_{b,1}$	3.6($/MW)	$\xi_{b,2}$	100($)	$H_{b,\text{med}}$	40(MW)
	$H_{b,\max}$	55(MW)	$v_{b,0}$	-0.25	$v_{b,1}$	2.33	$v_{b,2}$	-0.27
	v_b	0.15						
WPP	$\xi_{g,0}$	171.227($/MW)						
HESs	$H_{k,\text{rated}}$	3(MW)	$S_{k,\max}$	30(MW)	T_k	20(year)	β_k	0.99
	$\xi_{k,0}$	10($/MW)	$\xi_{k,1}$	8000($/MW)	$\xi_{k,2}$	4000($/MW)		
BES	$P_{q,\text{rated}}$	5(MW)	$S_{q,\max}$	55(MW)	T_k	20(year)	β_q	0.95
	$\xi_{q,0}$	26($/MW)	$\xi_{q,1}$	15000($/MW)	$\xi_{q,2}$	7000($/MW)		
DEHSs	ξ_t^{a}(Peak)	77($/MW)	ξ_t^{a}(Valley)	46($/MW)	ξ_t^{b}(Peak)	30($/MW)	ξ_t^{b}(Valley)	15($/MW)
	ξ_t^{c}	92($/MW)	ξ_t^{d}	7.7($/MW)	$P_{x,n,\min}$	0(MW)	$P_{x,n,\max}$	1(MW)
	$\delta_{x,n,\text{down}}$	0	$\delta_{x,n,\text{up}}$	0.2	$\beta_{x,n}$	0.99		

The comparison and specification of the three cases are shown in Table 3.

1) COMPARISON OF ELECTRIC POWER OPTIMAL SCHEDULING RESULTS

The scheduling results depicting the electric power output of generator units and BES for the three cases are exhibited in Figure 7 and Tables 4, 5, 6. In the tables, the negative and positive values for BES represent charging and discharging, respectively. The aggregate scheduling of electric power from HPPs, CHPs, WPP, and BES is observed to surpass the electric load demand in every instance, with the excess being attributed to wind power. However, the implementation of DEHS energy allocation scheduling in Cases 2 and 3, achieved by synchronizing the DEHS start-up time with WPP's output wind power, results in different patterns. Notably, Case 3 exhibits the highest consumption of WPP wind power during the scheduling periods of 1:00-7:00, whereas Case 1 displays the lowest. Additionally, constraints pertaining to operating costs, heat load demands, and the capacity of individual energy storage units within the scheduling model contribute to variations in the scheduled power of HPPs, CHPs, and BES. Therefore, a horizontal analysis is conducted to compare the scheduled electric power of these units across each moment, revealing the disparities and advantages of the scheduling strategies employed in the three cases.

The scheduling electric power of HPPs for three cases is shown in Figure 8. Given the constraints posed by operating costs, heat load demand, and the output wind power of WPP, both HPP_1 and HPP_2 operate at their minimum output power in all three cases. Additionally, during the scheduling periods of 1:00-9:00 and 17:00-24:00, the combined electric power output of $HPP_1 + HPP_2$ fluctuates to reflect changes in the electric load due to the decreased demand for electric load and the increasing output of wind power. This synchronicity creates an opportunity to accommodate additional wind power. The electric power output of the HPP_1 and HPP_2 remains consistent across the three cases, which can be obtained from Tables 4-6.

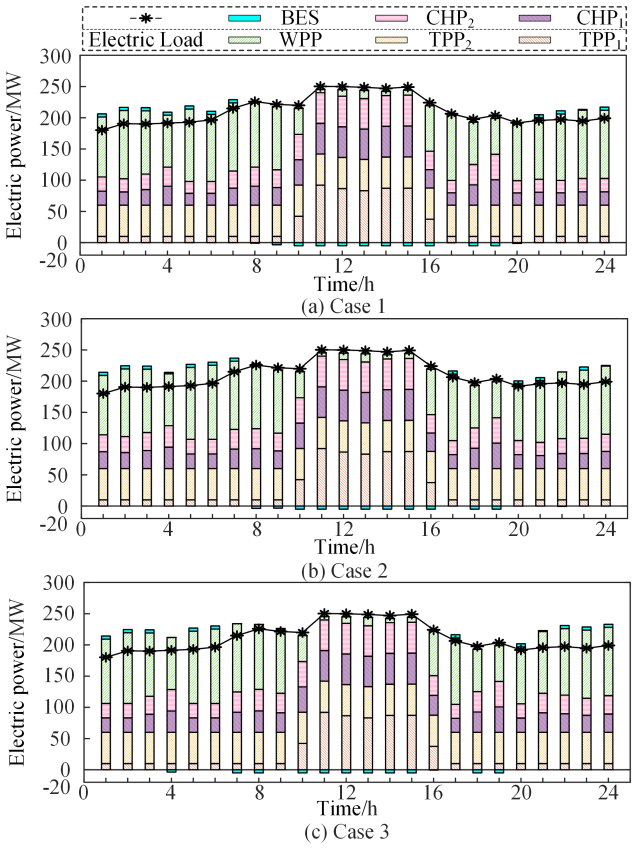

FIGURE 7. The scheduling results of electric power for three cases.

TABLE 3. Comparison and specification of the three cases.

Comparison	Case 1	Case 2	Case 3
Method	Traditional time-of-use electricity pricing scheduling strategy	EEAS	IEAS
Objective	min(38)	min(38)	min(38)
	The calculation in eqn (38) includes eqns (1), (12), (15), (16), (28), and (30).		
Constraints	In eqn (1) $C^{b}_{x,n,t} = C^{c}_{x,n,t} = C^{d}_{x,n,t} = 0$	In eqn (1) $C^{d}_{x,n,t} = 0$	Not limited
	(8), (13), (14), (17)-(27)	(6), (8), (13), (14), (17)-(27)	(6)-(11), (13), (14), (17)-(27)
	(29), (31)-(37), (39), (40)	(29), (31)-(37), (39), (40)	(29), (31)-(37), (39), (40)
Scheduling deviation $\Delta\delta_{x,n}$	Scheduling deviation is not considered.	0	0.2

TABLE 4. The electric power scheduling results of case 1.

Units	1	2	3	4	5	6	7	8	9	10	11	12	13	14	15	16	17	18	19	20	21	22	23	24/h
Electric load/MW	180.3	190.6	190.2	191.5	193	196.5	215	225.9	221.5	220	250.3	250	248.8	247.1	249.2	224.2	206.4	197.9	203.8	191.9	195.7	197.2	194.8	199.2
BES/MW	5	5	5	4.7	5	5	5	-0.8	-3.3	-5	-5	-5	-5	-5	-5	-5	-0.2	-5	-5	-1.3	4.6	5	1.4	4.9
WPP/MW	96	109.2	101.4	83.2	116	107.5	109.2	104	101.4	41.6	5.2	10.4	13	6.5	7.8	72.8	106.6	67.6	57.2	91.3	98.8	106.6	109.2	109.2
CHP_2/MW	22.6	21.2	24.9	30.5	19	19	27.4	30.5	28.4	40.6	49	49	48.8	49.2	49.6	29.5	19.8	32.7	40.8	19.7	20.8	19.8	21.5	21.5
CHP_1/MW	22.6	21.2	24.9	30.5	19	19	27.4	30.5	28.4	40.6	49	49	48.8	49.2	49.6	29.5	19.8	32.7	40.8	19.7	20.8	19.8	21.5	21.5
HPP_2/MW	50	50	50	50	50	50	50	50	50	50	50	50	50	50	50	50	50	50	50	50	50	50	50	50
HPP_1/MW	10	10	10	10	10	10	10	10	10	42.3	92.1	86.5	83.2	87.1	87.3	37.5	10	10	10	10	10	10	10	10

TABLE 5. The electric power scheduling results of case 2.

Units	1	2	3	4	5	6	7	8	9	10	11	12	13	14	15	16	17	18	19	20	21	22	23	24/h
Electric load/MW	180.3	190.6	190.2	191.5	193	196.5	215	225.9	221.5	220	250.3	250	248.8	247.1	249.2	224.2	206.4	197.9	203.8	191.9	195.7	197.2	194.8	199.2
BES/MW	5	5	5	2.4	5	5	5	-3.8	-3.3	-5	-5	-5	-5	-5	-5	-5	5	-5	-5	4.3	5	-0.5	5	1
WPP/MW	96	109.2	101.4	83.2	116	118.6	109.2	104	101.4	41.6	5.2	10.4	13	6.5	7.8	72.8	106.6	67.6	57.2	91.3	98.8	106.6	109.2	109.2
CHP_2/MW	27.1	25.7	28.9	34.3	23.4	23.4	31.4	32	28.4	40.6	49	49	48.8	49.2	49.6	29.5	22.4	32.7	40.8	22.5	21	24.1	24.3	27.5
CHP_1/MW	27.1	25.7	28.9	34.3	23.4	23.4	31.4	32	28.4	40.6	49	49	48.8	49.2	49.6	29.5	22.4	32.7	40.8	22.5	21	24.1	24.3	27.5
HPP_2/MW	50	50	50	50	50	50	50	50	50	50	50	50	50	50	50	50	50	50	50	50	50	50	50	50
HPP_1/MW	10	10	10	10	10	10	10	10	10	42.3	92.1	86.5	83.2	87.1	87.3	37.5	10	10	10	10	10	10	10	10

TABLE 6. The electric power scheduling results of case 3.

Units	1	2	3	4	5	6	7	8	9	10	11	12	13	14	15	16	17	18	19	20	21	22	23	24/h
Electric load/MW	180.3	190.6	190.2	191.5	193	196.5	215	225.9	221.5	220	250.3	250	248.8	247.1	249.2	224.2	206.4	197.9	203.8	191.9	195.7	197.2	194.8	199.2
BES/MW	5	5	5	0.6	5	5	5	-2.1	-2.9	-5	-5	-5	-5	-5	-5	-5	5	-5	-5	5	-1.3	2.8	5	2.9
WPP/MW	103	113.3	101.4	83.2	116	119.2	109.2	104	101.4	41.6	5.2	10.4	13	6.5	7.8	72.8	106.6	67.6	57.2	91.3	98.8	106.6	109.2	109.2
CHP_2/MW	23.2	23.2	28.9	36.4	23.2	23.2	28.4	32.9	28.6	40.6	49	48.9	48.6	49.6	49.6	32.5	27.2	32.7	40.8	27	28.1	28	27.3	27.9
CHP_1/MW	23.2	23.2	28.9	36.4	23.2	23.2	28.4	32.9	28.6	40.6	49	48.9	48.6	49.6	49.6	32.5	27.2	32.7	40.8	27	28.1	28	27.3	27.9
HPP_2/MW	50	50	50	50	50	50	50	50	50	50	50	50	50	50	50	50	50	50	50	50	50	50	50	50
HPP_1/MW	10	10	10	10	10	10	10	10	10	42.3	92.1	86.5	83.2	87.1	87.3	37.5	10	10	10	10	10	10	10	10

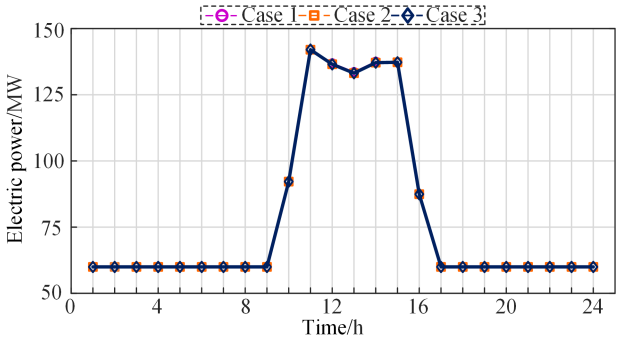

FIGURE 8. The scheduling electric power of HPPs for three cases.

The comparison of CHP scheduling electric power across the three cases is presented in Figure 9. With variations in wind power, the operational time and energy storage periods of DEHS are reallocated to periods without wind curtailment. While the time-of-use scheduling strategy of Case 1 is influenced by both wind power output and system operational costs, it does not schedule all DEHSs to reduce costs when wind power decreases, such as at 4:00, in order to meet electric load demand and accommodate wind power. Therefore, Figure 9 reveals that the CHP scheduling power curve is higher in Cases 2 and 3 than in Case 1 during each scheduling period. Additionally, compared to Case 2, due to the increased scheduling power of DEHS based on EEAS in Case 3, the combined power of $CHP_1 + CHP_2$ in Case 3 is more significant than in Case 2 from 3:00 to 24:00. These results suggest that implementing energy allocation for DEHS enhances the flexibility of CHP regulation.

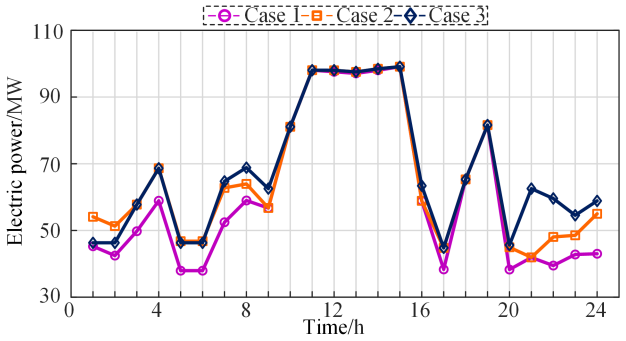

FIGURE 9. The simulation results of CHPs scheduling electric power for three cases.

2) COMPARISON OF HEAT POWER OPTIMAL SCHEDULING RESULTS

The simulation results of the heat power output of CHPs and HESs across three cases are exhibited in Figure 10 and Tables 7, 8, 9. In the tables, the negative and positive values for HES represent charging and discharging, respectively. It is evident that, in all three cases, the scheduled heat power generated by CHPs, HESs, and DEHS is sufficient to fulfil the heat load demand. Notably, during the scheduling period of 8:00-15:00, when the wind power output from the WPP decreases, CHPs refrain from reducing their output to enhance the grid's accommodation capacity for wind power. Therefore, the heat power scheduling for each unit remains stable within this period, as depicted in Figure 10. However, the variations in heat power during other scheduling periods are influenced by the different scheduling strategies employed in each case. Specifically, in Case 2, the DEHS solely consumes electrical energy to generate heat for user heating without assisting in district heating network regulation. Conversely, in Cases 1 and 3, the heat energy stored in DEHS of users in urban areas is released into the district heating network to facilitate heat network regulation. Notably, Case 3's heat power scheduling is smaller than Case 1's since IEAS schedules extra user demand heat energy in Case 3, whereas DEHS reacts to the grid in Case 1. These scheduling results underscore the DEHS's ability to regulate the district heating network and further demonstrate that, compared to Case 1, Case 3 offers superior heat comfort for users.

The comparison of CHPs scheduling heat power for three cases is shown in Figure 11. Given that CHPs operate under backpressure steam conditions and are susceptible to the electric-heat coupling relationship among units, the electric power scheduling for CHPs in Cases 2 and 3 exceeds that of Case 1. Therefore, as reflected in Figure 11, the heat power curves scheduled for these two cases surpass those of Case 1. The scheduling results reveal that, in contrast to conventional scheduling strategies, the enhanced flexibility in regulating CHPs effectively addresses variable scenarios of wind power output from the WPP and fluctuations in load demand within the electric heat network.

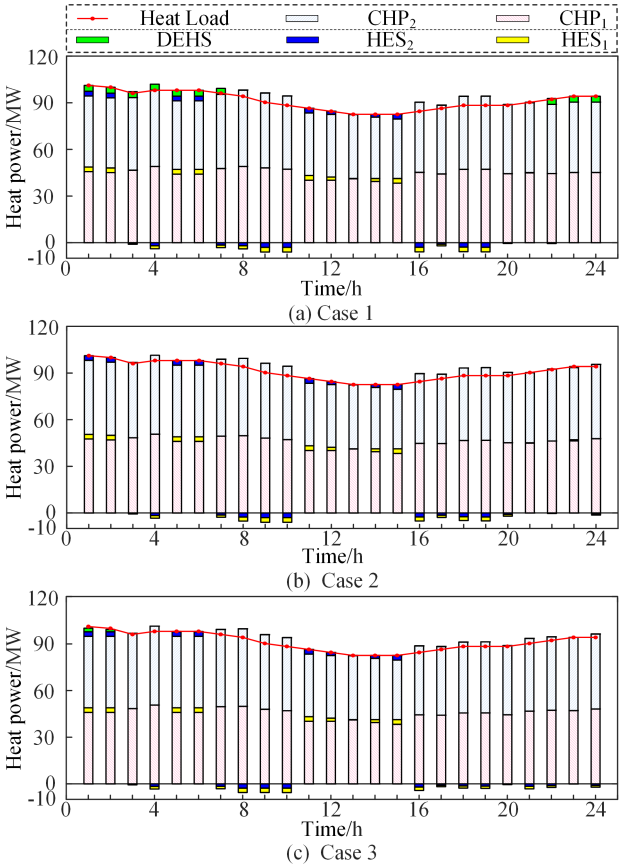

FIGURE 10. The simulation results of CHPs and HESs output heat power for three cases.

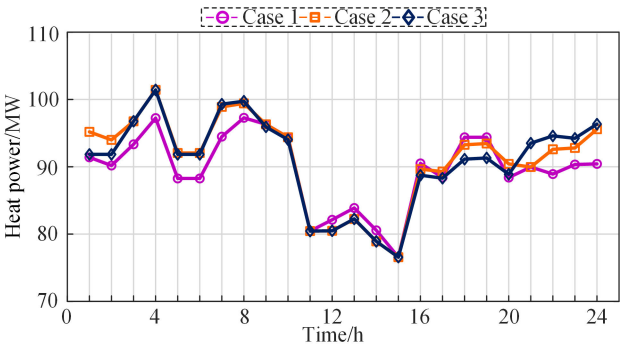

FIGURE 11. The comparison of CHPs scheduling heat power for three cases.

3) COMPARISON OF DEHS OPTIMAL SCHEDULING RESULTS

The predicted and scheduled power of DEHS in Case 1 is depicted in Figure 12. A comparison of the scheduled and predicted electric power for DEHS user 1 reveals that the former stands at 4×7 MW, while the latter amounts to 4×11 MW, as seen in Figure 6. In contrast, the scheduling power of DEHS user 2 is diminished by 4 MW at 6:00 when contrasted with the predicted power. Similarly, the scheduled electric power for DEHS user 3 is reduced by 4 MW at 4:00,

TABLE 7. The heat power scheduling results of case 1.

Units	1	2	3	4	5	6	7	8	9	10	11	12	13	14	15	16	17	18	19	20	21	22	23	24/h
Heat load/MW	101.2	100	96.1	98.1	98.1	98.1	96.1	94.1	90.3	88.4	86.5	84.5	82.6	82.6	82.6	84.5	86.5	88.4	88.4	88.4	90.3	92.3	94.2	94.2
DEHS/MW	3.8	3.8	3.8	3.8	3.8	3.8	3.8	0	0	0	0	0	0	0	0	0	0	0	0	0	0	3.8	3.8	3.8
HES_2/MW	3	3	-0.5	-1.9	3	3	-1.6	-2	-3	-3	3	2	0.2	1.8	3	-2.9	-1.1	-2.9	-2.9	-0.2	0.3	-0.3	0	0
CHP_2/MW	45.7	45.1	46.7	49.1	44.1	44.1	47.7	49.1	48.2	47.2	40.2	40.2	41.1	39.5	38.3	45.2	44.3	47.1	47.1	44.4	44.9	44.5	45.2	45.2
CHP_1/MW	45.7	45.1	46.7	49.1	44.1	44.1	47.7	49.1	48.2	47.2	40.2	40.2	41.1	39.5	38.3	45.2	44.3	47.1	47.1	44.4	44.9	44.5	45.2	45.2
HES_1/MW	3	3	-0.5	-1.9	3	3	-1.6	-2	-3	-3	3	2	0.2	1.8	3	-2.9	-1.1	-2.9	-2.9	-0.2	0.3	-0.3	0	0

TABLE 8. The heat power scheduling results of case 2.

Units	1	2	3	4	5	6	7	8	9	10	11	12	13	14	15	16	17	18	19	20	21	22	23	24/h
Heat load/MW	101.2	100	96.1	98.1	98.1	98.1	96.1	94.1	90.3	88.4	86.5	84.5	82.6	82.6	82.6	84.5	86.5	88.4	88.4	88.4	90.3	92.3	94.2	94.2
HES_2/MW	3	3	-0.3	-1.7	3	3	-1.4	-2.6	-3	-3	3	2	0.2	1.8	3	-2.6	-1.4	-2.4	-2.5	-1.1	0.2	-0.2	0.7	-0.7
CHP_2/MW	47.6	47	48.4	50.7	46	46	49.5	49.7	48.2	47.2	40.2	40.2	41.1	39.5	38.3	44.8	44.7	46.6	46.7	45.2	45	46.3	46.4	47.8
CHP_1/MW	47.6	47	48.4	50.7	46	46	49.5	49.7	48.2	47.2	40.2	40.2	41.1	39.5	38.3	44.8	44.7	46.6	46.7	45.2	45	46.3	46.4	47.8
HES_1/MW	3	3	-0.3	-1.7	3	3	2	0.2	1.8	3	3	2	0.2	1.8	3	-2.6	-1.4	-2.4	-2.5	-1.1	0.2	-0.2	0.7	-0.7

TABLE 9. The heat power scheduling results of case 3.

Units	1	2	3	4	5	6	7	8	9	10	11	12	13	14	15	16	17	18	19	20	21	22	23	24/h
Heat load/MW	101.2	100	96.1	98.1	98.1	98.1	96.1	94.1	90.3	88.4	86.5	84.5	82.6	82.6	82.6	84.5	86.5	88.4	88.4	88.4	90.3	92.3	94.2	94.2
DEHS/MW	2.2	1.4	0	0	0.1	0.1	0	0	0	0	0	0	0	0	0	0	0	0	0	0	0	0	0	0
HES_2/MW	3	3	-0.3	-2.6	3	3	-0.1	-3	-3	-3	3	1.4	-0.4	3	3	-2.2	-1.4	-1.4	-1.5	-0.9	-1.1	-0.8	-0.2	-0.6
CHP_2/MW	45.9	45.9	48.4	51.6	45.9	45.9	48.2	50.1	48.2	47.2	40.2	40.8	41.7	38.3	38.3	44.4	44.6	45.6	45.7	45.1	46.2	47	47.3	47.7
CHP_1/MW	45.9	45.9	48.4	51.6	45.9	45.9	48.2	50.1	48.2	47.2	40.2	40.8	41.7	38.3	38.3	44.4	44.6	45.6	45.7	45.1	46.2	47	47.3	47.7
HES_1/MW	3	3	-0.3	-2.6	3	3	-0.1	-3	-3	-3	3	1.4	-0.4	3	3	-2.2	-1.4	-1.4	-1.5	-0.9	-1.1	-0.8	-0.2	-0.6

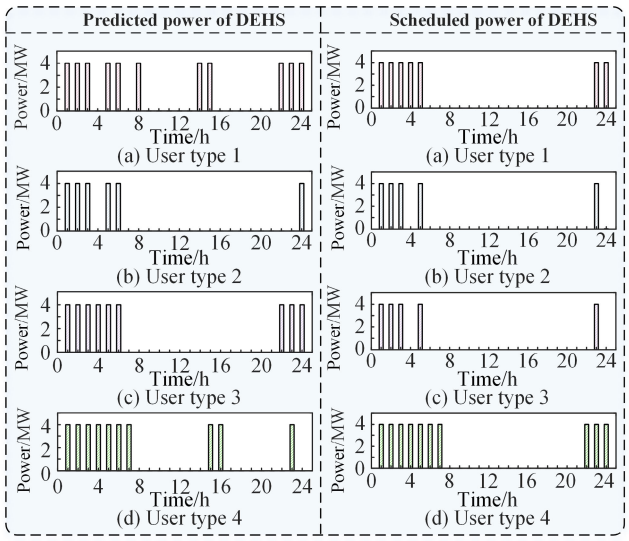

FIGURE 12. The predicted and scheduled power of DEHS in Case 1.

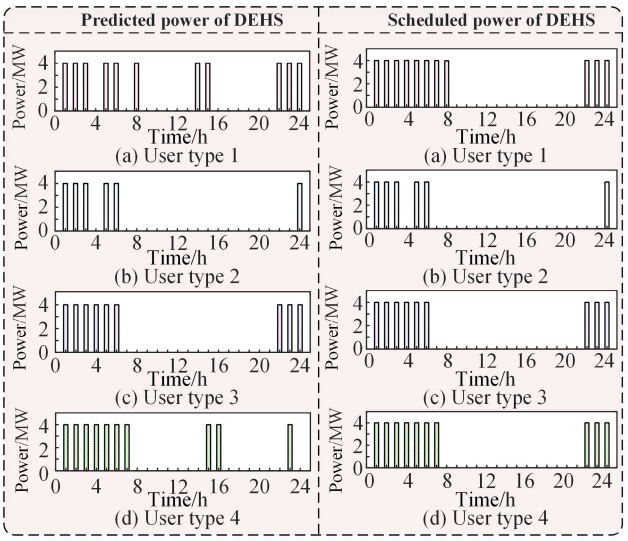

FIGURE 13. The predicted and scheduled power of DEHS in Case 2.

6:00, 22:00, and 24:00, respectively, in comparison to the predicted power. Notably, only for DEHS user type 4 does the scheduling power align with the predicted power. Therefore, comparing of the scheduling results across the four DEHS users indicates that the time-of-use based scheduling power falls short of meeting user demand.

The predicted and scheduled power of DEHS in Case 2 is presented in Figure 13. Given the reduced wind power output during the hours of 11:00 to 15:00, there is no WPC during this period. Therefore, the optimized scheduling for DEHS user 1 reallocates the working hours originally designated for energy utilization at 14:00 and 15:00 in Figure 6 to 4:00 and 7:00 in Figure 13. Similarly, the working hours for DEHS user 2 at 15:00 and 16:00 in Figure 6 are reallocated to 22:00 and 24:00 in Figure 13. Notably, the scheduling power for DEHS user 3 and 4 remains equivalent

to their predicted power, respectively. Overall, the total DEHS scheduling electric power in Case 2 aligns with the predicted power depicted in Figure 6. These findings demonstrate that, in comparison to EEAS with time-of-use scheduling, user demand can be effectively met, and wind power accommodation is enhanced during off-peak hours.

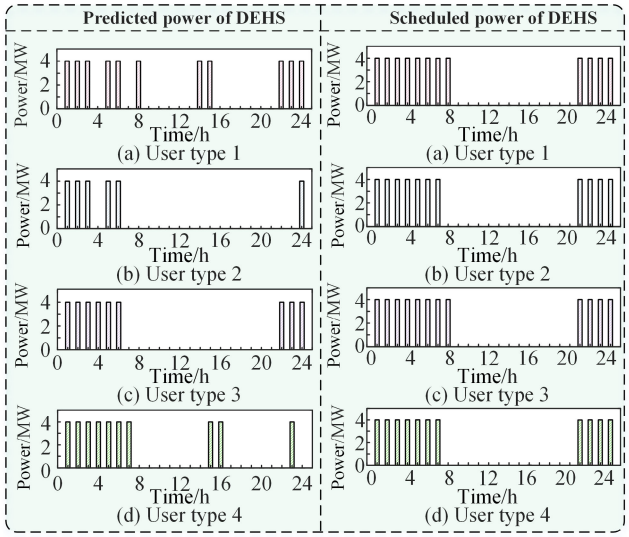

FIGURE 14. The predicted and scheduled power of DEHS in Case 3.

The predicted and scheduled power of DEHS in Case 3 is depicted in Figure 14. A comparison of the optimized scheduling results between IEAS in Figure 14 and EEAS in Figure 13 reveals several notable differences. Specifically, in Figure 14 (a), the scheduling power at 21:00 is augmented by 4 MW in comparison to Figure 13 (a). Similarly, in Figure 14 (b), the scheduling power is increased by 4 × 5 MW at 4:00, 7:00, and between 21:00 to 23:00, exceeding the corresponding levels in Figure 13 (b). Furthermore, Figure 14 (c) demonstrates an increase of 4 × 3 MW in scheduling power at 7:00, 8:00, and 21:00, surpassing the values observed in Figure 13 (c). Lastly, in Figure 14 (d), the scheduling power at 21:00 is elevated by 4 MW, exceeding the level shown in Figure 13 (d). These scheduling results clearly illustrate that, within the permitted regulation margin, the IEAS adjusts the working hours to fluctuations in wind power, thereby enhancing the flexibility of DEHS scheduling and optimizing wind power accommodation.

According to the scheduling results in Figures 13 and 14, the deviation $\delta_{x,n}$ in Cases 2 and 3 are 0 and 0.2, respectively. To analyze the impact of $\delta_{x,n}$ on the depth of grid regulation, the contribution value of the DEHS to the grid regulation of wind power accommodation is obtained, the evaluation index ϑ for Cases 2 and 3 are 2.07% and 2.63%, respectively. These two indices represent the ratio of the wind power accommodated by DEHS through the application of EEAS and IEAS strategies, compared to the baseline wind power accommodation capacity. Compared with Case 2, Case 3 can provide 27.05% more scheduling space for the grid to consume wind power when the DEHS simulation capacity is the same. The proposed IEAS optimized scheduling strategy can effectively increase the accommodation of wind power, which is beneficial for both grid operators and the wind power industry.

4) COMPARISON OF WPC AND OPERATING COSTS

The curves depicting the predicted and scheduled wind power for the three cases are presented in Figure 15. Notably, during the 1:00-3:00 period, the absorbed wind power in Case 3 surpasses that of Cases 1 and 2. Similarly, in the 5:00-7:00 period, both Cases 3 and 2 exhibit higher wind power accommodation than Case 1. The hierarchy of wind power accommodation among the three cases stands as follows: Case 3 > Case 2 > Case 1. This finding further attests to the efficacy of the energy allocation strategy employed within DEHS.

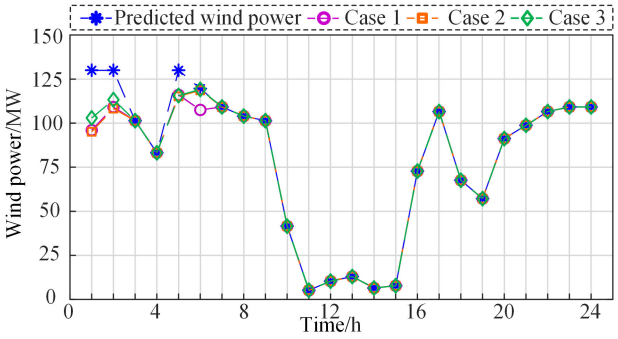

FIGURE 15. The curves of predicted and scheduled wind power for three cases.

The comparison of simulation results for three cases is presented in Table 10.

TABLE 10. The comparison of costs and WPC rates for three cases.

Costs and WPC rate	Case 1	Case 2	Case 3
Total cost/$	90,613.56	93,805.63	97,224.03
Operation cost/$	73,461.01	73,829.58	74,059.21
WPC cost/$	10,970.17	9,812.56	7,932.34
DEHS cost$	6,182.38	10,163.49	15,232.48
WPC rate/%	3.56	3.06	2.51

In Case 1, the scheduling of DEHS is solely based on time-of-use, determining its operating cost exclusively through peak and valley prices. Conversely, in Cases 2 and 3, the energy allocation strategy of DEHS is implemented, incorporating subsidies provided by the grid to users in the calculation of operating costs. Therefore, the total operating costs reported in Table 10 for Cases 2 and 3 exceed those of Case 1. Furthermore, the implementation of IEAS in Case 3 results in a higher scheduling of wind power and a more significant regulation of DEHS by the grid. This leads to increased subsidies from the grid to users in Case 3 compared to Case 2. Despite the higher operating costs in Cases 2 and 3,

the WPC rates for these cases are reduced by 14.04% and 29.49%, respectively.

Specifically, it is emphasized that the costs of the user and system operator in this paper are not distinguished. The cost of DEHS is incorporated into the overall consideration. The DEHS costs for the three cases in Table 10 are 6,182.38 $, 10,163.49 $, and 15,232.48 $, respectively. The scheduling cost of DEHS is gradually increasing, thereby raising total costs. Suppose the costs of users and system operators are separated, and the DEHS cost excludes the electricity cost of users. In that case, the total cost of the proposed method decreases, which can be proved by the decrease in the wind penalty cost for the three cases as shown in Table 10, where the WPC costs are 10,970.17 $, 9,812.56 $, and 7,932.34 $, respectively. This study demonstrates that the optimized scheduling of combined electricity and heat systems with DEHS, without the distinction between user and system operator costs, can be reduced in terms of WPC. With regard to distinguishing between the profit of users and system operators, this will be taken as a basis, leveraging the energy allocation of DEHS as an auxiliary service for electricity market trading.

VI. CONCLUSION

An optimal scheduling strategy for energy allocation of DEHS is proposed to enhance the accommodation of wind power. DEHS is widely distributed on the load side, and the diverse heat demand of users needs to be taken into account. Therefore, the heat comfort of DEHS users and their willingness to serve the grid are considered, and the energy allocation strategy is further divided into EEAS and IEAS. The proposed energy allocation strategy is verified using a 6-bus system. The general model of energy allocation can reallocate the working time of DEHS according to the variation of wind power.

The study is compared by three simulation cases. Compared with the conventional scheduling strategy of time-of-use, the WPC rate of EEAS is reduced by 14.04%, and the WPC rate of IEAS is reduced by 29.49%. The evaluation index ϑ for EEAS and IEAS is 2.07% and 2.63%, respectively. IEAS can provide 27.05% more scheduling space for the grid to consume wind power compared to EEAS. Grid regulatory flexibility is enhanced by the energy allocation of DEHS, and the WPC is reduced, which is beneficial for both grid operators and the wind power industry.

This study mainly focuses on the energy allocation of DEHS. However, the system may encounter more complex factors, such as changes in user demand, fluctuations in electricity prices, and other factors that could potentially affect the strategy. Based on the potential limitations of this study, an interesting direction is open for future study. To further explore the economic aspects of this method and consider the impact of multiple factors on scheduling strategies, the energy allocation of DEHS is traded as an auxiliary service in the electricity market.

REFERENCES

[1] J. Li, J. Zhou, and B. Chen, "Review of wind power scenario generation methods for optimal operation of renewable energy systems," *Appl. Energy*, vol. 280, Dec. 2020, Art. no. 115992, doi: 10.1016/j.apenergy.2020.115992.

[2] M. Ali, M. A. Abdulgalil, I. Habiballah, and M. Khalid, "Optimal scheduling of isolated microgrids with hybrid renewables and energy storage systems considering demand response," *IEEE Access*, vol. 11, pp. 80266–80273, 2023, doi: 10.1109/ACCESS.2023.3296540.

[3] Y. Song and L. Shi, "Dynamic economic dispatch with CHP and wind power considering different time scales," *IEEE Trans. Ind. Appl.*, vol. 58, no. 5, pp. 5734–5746, Sep. 2022, doi: 10.1109/TIA.2022.3188603.

[4] G. Buttitta, C. N. Jones, and D. P. Finn, "Evaluation of advanced control strategies of electric thermal storage systems in residential building stock," *Utilities Policy*, vol. 69, Apr. 2021, Art. no. 101178, doi: 10.1016/j.jup.2021.101178.

[5] W. Zheng, Y. Wang, C. Li, J. Li, X. Wang, L. Zhang, and R. Lin, "Study on the thermal storage performance of a new electric heating device with phase change materials," *J. Energy Storage*, vol. 56, Dec. 2022, Art. no. 105981, doi: 10.1016/j.est.2022.105981.

[6] H. Ji, J. Yang, H. Wang, K. Tian, M. O. Okoye, and J. Feng, "Electricity consumption prediction of solid electric thermal storage with a cyber–physical approach," *Energies*, vol. 12, no. 24, p. 4744, Dec. 2019, doi: 10.3390/en12244744.

[7] H. Wang, J. Han, R. Zhang, M. Sun, Z. Sun, P. Hua, Z. Xie, H. Wang, E. Abdollahi, R. Lahdelma, K. Granlund, and E. Teppo, "Heat-power peak shaving and wind power accommodation of combined heat and power plant with thermal energy storage and electric heat pump," *Energy Convers. Manage.*, vol. 297, Dec. 2023, Art. no. 117732, doi: 10.1016/j.enconman.2023.117732.

[8] J. Wang, S. You, Y. Zong, C. Træholt, Z. Y. Dong, and Y. Zhou, "Flexibility of combined heat and power plants: A review of technologies and operation strategies," *Appl. Energy*, vol. 252, Oct. 2019, Art. no. 113445, doi: 10.1016/j.apenergy.2019.113445.

[9] B. Qu, L. Fu, and Z. Xing, "Research on collaborative optimal dispatching of electric heating integrated energy based on wind power prediction accuracy," *IEEE Access*, vol. 11, pp. 145167–145184, 2023, doi: 10.1109/ACCESS.2023.3344178.

[10] J. R. Eggers, M. von der Heyde, S. H. Thaele, H. Niemeyer, and T. Borowitz, "Design and performance of a long duration electric thermal energy storage demonstration plant at megawatt-scale," *J. Energy Storage*, vol. 55, Nov. 2022, Art. no. 105780, doi: 10.1016/j.est.2022.105780.

[11] Q. Ji, Z. Han, X. Li, and L. Yang, "Energy and economic evaluation of the air source hybrid heating system driven by off-peak electric thermal storage in cold regions," *Renew. Energy*, vol. 182, pp. 69–85, Jan. 2022, doi: 10.1016/j.renene.2021.10.026.

[12] S. Oh, B. S. Oh, and J. I. Lee, "Performance evaluation of supercritical carbon dioxide recompression cycle for high temperature electric thermal energy storage," *Energy Convers. Manage.*, vol. 255, Mar. 2022, Art. no. 115325, doi: 10.1016/j.enconman.2022.115325.

[13] C. Srithapon and D. Månsson, "Predictive control and coordination for energy community flexibility with electric vehicles, heat pumps and thermal energy storage," *Appl. Energy*, vol. 347, Oct. 2023, Art. no. 121500, doi: 10.1016/j.apenergy.2023.121500.

[14] Z. Rostamnezhad, N. Mary, L.-A. Dessaint, and D. Monfet, "Electricity consumption optimization using thermal and battery energy storage systems in buildings," *IEEE Trans. Smart Grid*, vol. 14, no. 1, pp. 251–265, Jan. 2023, doi: 10.1109/TSG.2022.3194815.

[15] H. Ji, H. Wang, J. Yang, J. Feng, Y. Yang, and M. O. Okoye, "Optimal schedule of solid electric thermal storage considering consumer behavior characteristics in combined electricity and heat networks," *Energy*, vol. 234, Nov. 2021, Art. no. 121237, doi: 10.1016/j.energy.2021.121237.

[16] H. Wang, J. Yang, Z. Chen, G. Li, J. Liang, Y. Ma, H. Dong, H. Ji, and J. Feng, "Optimal dispatch based on prediction of distributed electric heating storages in combined electricity and heat networks," *Appl. Energy*, vol. 267, Jun. 2020, Art. no. 114879, doi: 10.1016/j.apenergy.2020.114879.

[17] L. Gomes and Z. Vale, "Costless renewable energy distribution model based on cooperative game theory for energy communities considering its members' active contributions," *Sustain. Cities Soc.*, vol. 101, Feb. 2024, Art. no. 105060, doi: 10.1016/j.scs.2023.105060.

[18] P. Zare, A. Dejamkhooy, and I. F. Davoudkhani, "Efficient expansion planning of modern multi-energy distribution networks with electric vehicle charging stations: A stochastic MILP model," *Sustain. Energy, Grids Netw.*, vol. 38, Jun. 2024, Art. no. 101225, doi: 10.1016/j.segan.2023.101225.

[19] R. Talat, M. Muzammal, Q. Qu, W. Zhou, M. Najam-ul-Islam, S. M. H. Bamakan, and J. Qiu, "A decentralized system for green energy distribution in a smart grid," *J. Energy Eng.*, vol. 146, no. 1, Feb. 2020, Art. no. 0000623, doi: 10.1061/(asce)ey.1943-7897.0000623.

[20] H.-S. Ahn, B.-Y. Kim, Y.-H. Lim, B.-H. Lee, and K.-K. Oh, "Distributed coordination for optimal energy generation and distribution in cyber-physical energy networks," *IEEE Trans. Cybern.*, vol. 48, no. 3, pp. 941–954, Mar. 2018, doi: 10.1109/TCYB.2017.2669041.

[21] H. Yang, Y. Zhang, Y. Ma, M. Zhou, and X. Yang, "Reliability evaluation of power systems in the presence of energy storage system as demand management resource," *Int. J. Electr. Power Energy Syst.*, vol. 110, pp. 1–10, Sep. 2019, doi: 10.1016/j.ijepes.2019.02.042.

[22] M. Liu, H. Zheng, and L. Qin, "Research on the collaborative scheme of integrated peak-regulation resources based on generation-grid-load-storage," in *Proc. 12th IEEE PES Asia–Pacific Power Energy Eng. Conf. (APPEEC)*, Sep. 2020, pp. 1–5, doi: 10.1109/APPEEC48164.2020.9220342.

[23] Y. Dai, L. Chen, Y. Min, Q. Chen, J. Hao, K. Hu, and F. Xu, "Dispatch model for CHP with pipeline and building thermal energy storage considering heat transfer process," *IEEE Trans. Sustain. Energy*, vol. 10, no. 1, pp. 192–203, Jan. 2019, doi: 10.1109/TSTE.2018.2829536.

[24] Z. Li, W. Wu, J. Wang, B. Zhang, and T. Zheng, "Transmission-constrained unit commitment considering combined electricity and district heating networks," *IEEE Trans. Sustain. Energy*, vol. 7, no. 2, pp. 480–492, Apr. 2016, doi: 10.1109/TSTE.2015.2500571.

[25] Y. Fang, S. Zhao, N. Wang, Z. Li, and J. Liu, "Power system stochastic optimal dispatch considering thermal and electrical coordination," *Int. J. Electr. Power Energy Syst.*, vol. 110, pp. 772–780, Sep. 2019, doi: 10.1016/j.ijepes.2019.03.065.

HUICHAO JI received the B.S. degree in measurement and control technology and instruments from Jilin Institute of Chemical Technology, Jilin, China, in 2010, the M.S. degree in control engineering from Northeast Electric Power University, Jilin, in 2015, and the Ph.D. degree in electrical engineering from Shenyang University of Technology, Shenyang, China, in 2022. He is currently a Lecturer with Northeast Electric Power University, Jilin. His research interests include smart grids, power system optimization, and electric and thermal energy storage technology.

LEI WANG received the B.S. and M.S. degrees in electronic information engineering from China University of Petroleum, Beijing, China, in 2006 and 2011, respectively. She is currently an Associate Professor with Jilin Institute of Chemical Technology, Jilin, China. Her research interests include power system optimization, image and signal processing, and algorithm optimization.